

Optical Spectra and Interfacial Band Offsets of Pulse-Laser-Deposited Metal-Oxides: SnO₂, TiO₂, and ZnO

Nhan V. Nguyen,^{1,*} Nam Nguyen,^{2,*} Jason R. Hatrick-Simpers,² Oleg A. Kirillov,¹ and Martin L. Green²

¹Nanoscale Device Characterization Division

²Materials Measurement Science Division

National Institute of Standards and Technology, Gaithersburg, Maryland 20899, USA

*These authors contributed equally to this work.

Contacts: Nhan.Nguyen@nist.gov

ABSTRACT

Transparent conducting oxides are electrically conductive materials with high optical transmittance in the visible region of the spectrum and are useful in a wide range of applications. In this study, the optical spectra of a set of single-phase transparent conducting oxides TiO₂, ZnO, and SnO₂ grown by pulse laser deposition are measured by vacuum ultra-violet spectroscopic ellipsometry (SE) and the optical band gaps are determined to be 3.30 ± 0.05 eV, 3.13 ± 0.05 eV, and 3.95 ± 0.05 eV, respectively. Differences between these values and previous measurements are discussed. SnO₂ and ZnO optical responses at the band gap reveal that they are a direct band gap while TiO₂ appears to show an indirect type. For the interfacial electronic characteristics, internal photoemission (IPE) measurement shows that the electronic barriers of these naturally *n*-type doped metal oxides adjacent to an Al₂O₃ layer originate from the Fermi level in their conduction bands. The band offset determination shows the barrier heights are similar and have small internal field dependence. The work functions are then estimated from the measured barrier heights.

Transparent conducting oxides (TCOs) used as transparent electrodes are found in many critical components in modern electronic and optoelectronic devices.¹ The fast-growing use of TCO and the associated high cost of fabrication have resulted in a topic of intense research to improve the performances, to reduce the cost, and to explore many potential opportunities for future applications. As the name TCO suggests, two intuitively contradictory properties are the high optical transmittance (insulator-like) in the visible and near-infrared spectral range and the high electrical conductivity (metal-like).^{2,3} These two key properties have generated many application opportunities for novel devices in thin film solar cells, flat panel displays, light-emitting devices, or heated windows. To be transparent in the visible spectral range, it is required that TCOs must possess a wide bandgap of greater than 3.0 eV and at the same time, must have high carrier concentration and high mobility by native or substitutional dopants. Researchers have been exploring many old and new TCO materials with the aim to achieve critical optical and electrical properties relevant to some specific application. The realization of a desired material is contingent on the understanding and knowledge of structural, electronic, and optical properties and their interfacing characteristics with other materials inside the devices. Despite their appeal and widespread uses, many fundamental optoelectronic properties of these materials remain currently not well understood. For instance, material parameters such as optical transmittance and electronic interfacial characteristics still need to be accurately characterized and determined to optimize the design and performance of a device. It is also important to obtain high quality single phase thin films to properly characterize these material parameters for future TCO device applications.

Currently, the most investigated and technically used TCO materials are indium oxide (IO), tin-doped indium oxide (ITO), zinc oxide (ZnO), tin oxide (SnO₂), and, titanium oxide (TiO₂).⁴ In this letter, we report an investigation on some of the fundamental optoelectronic properties of three different transparent metal oxides, SnO₂, TiO₂, and ZnO, fabricated by pulse laser deposition (PLD).⁵ Spectroscopic ellipsometry (SE) is employed to provide optical properties.⁶ The dielectric functions, absorptions, and optical band gaps will be determined and examined. The conduction band minimum (CBM) depth or electron affinity which affects the doping likelihood of TCOs, is also equally important in determining the conducting properties. A higher value of electron affinity would facilitate the process of introducing charge carriers.⁷ The energy barriers were examined by using a robust technique of internal photoemission (IPE)⁸. This reveals the electronic characteristics at the interface that might provide some understanding of their optical and electrical interfacial properties.

SnO₂, TiO₂, and ZnO films were grown on *c*-plane sapphire (Al₂O₃) substrate by PLD using KrF excimer laser ($\lambda=248$ nm). High-purity (99.9%) ZnO, TiO₂ and SnO₂ polycrystalline targets were used to

grow thin films for structural determination and optoelectrical measurements. The PLD deposition was conducted at substrate temperature of 600 °C and O₂ partial pressure of 1x10⁻³ Torr. The targets were ablated using a laser power density of 3 J/cm² and laser frequency rate of 5 Hz. The structural quality of the films was examined by X-ray diffraction (XRD) on Bruker D8 diffractometer equipped with Cu K α and high-resolution two-dimensional (2D) detector. Fig. 1(a) shows 2D XRD image of the oxide films measured over 2 θ = 30° to 60° range. The 2D XRD image shows only strong diffraction from rutile TiO₂ (200), rutile SnO₂ (200) and hexagonal wurtzite ZnO (0002) at 2 θ = 39.5°, 38.6° and 34.4°, respectively. XRD measurements detected no secondary crystal phases from the oxide films. This demonstrates all films were highly-oriented and/or epitaxially grown on Al₂O₃ substrate. Here, it is worth noting that all the films were unintentionally doped. On the bare surface of these metal oxide films/substrate, ellipsometry measurements were performed by using a vacuum ultra-violet spectroscopic ellipsometer with light photon energy range from 1.0 eV to 8.0 eV. A series of metal/high-*k* dielectric/TCO structures, schematically displayed in Fig. 1(b), were fabricated for IPE measurements. Briefly, the metal oxide layer (TiO₂, ZnO, and SnO₂) was deposited on top of a RuO₂ layer which was ~~also~~ PLD grown on sapphire substrate. RuO₂ was used as an electrical back contact for IPE measurement due to the fact that it exhibits high electrical conductivity at room temperature and it has a rutile structure that is similar to TiO₂ and SnO₂ ($a_{\text{RuO}_2} = 0.450$ nm, $a_{\text{TiO}_2} = 0.459$ nm, and $a_{\text{SnO}_2} = 0.474$ nm). Additionally, atomic arrangements of the (010) SnO₂ plane have very good structural compatibility with that of the (0-110) ZnO plane thus enabling the epitaxial and/or lattice-matched growth of TiO₂, SnO₂ and ZnO directly onto RuO₂/Al₂O₃ substrate for this study. A high-*k* Al₂O₃ insulator was deposited on top of the metal oxide by atomic-layer deposition (ALD) to a thickness of 30 nm. A top aluminum (Al) electrode was deposited by electron evaporation to a thickness of 15 nm, which is thin enough to allow the IPE incident light to penetrate and reach the underneath metal oxide layer. The photocurrent, I_g , was measured as a function of photon energy from 1.5 eV to 5.0 eV with the applied gate bias, V_g , varied from -3.0 to 3.0 V in steps of 0.1 V. The IPE quantum yield (Y) is defined as a ratio of photocurrent and incident photon flux.⁹ The aim of IPE measurements is to obtain the electronic barrier height at the buried metal oxide / Al₂O₃ interface.

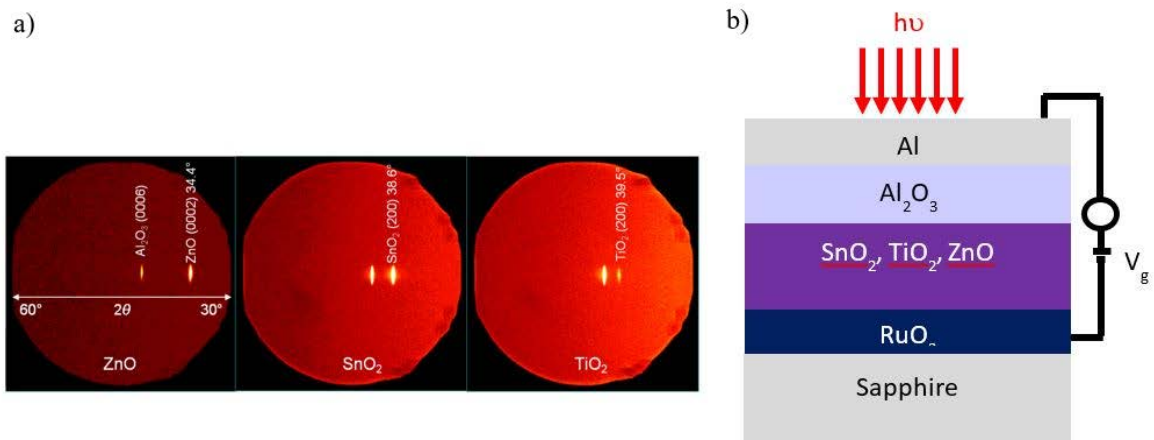


Fig. 1: (a) XRD images of ZnO, SnO₂, TiO₂ and, and (b) Schematic structure of the samples and internal photoemission measurement

From SE measurements, the complex pseudo-dielectric functions, $\langle \epsilon \rangle = \langle \epsilon_1 \rangle + j \langle \epsilon_2 \rangle = (\langle n \rangle + j \langle k \rangle)^2$ were obtained as shown in Fig. 2 where n and k are the index of refraction and extinction coefficient. The dielectric function of TiO_2 is much higher than those of ZnO and SnO_2 implying TiO_2 has a higher electron affinity and polarizability. There have been many published reports on the experimental and theoretical studies of optical properties of these materials in the bulk form or thin film grown by a variety of different techniques. Our PLD films have similar index of refraction compared with those prepared by other deposition techniques. In general, naturally or intentionally doped metal oxides behave electrically like metals at room temperature and exhibit a high optical transparency in the visible spectrum. The dielectric functions displayed in Fig. 2 show that these metal oxides are optically transparent below ~ 3.0 eV or above ~ 400 nm. There is only one excitonic feature near the absorption edge (3.3 eV for ZnO , 4.4 eV for TiO_2 , and 4.0 eV for SnO_2 , see $\langle \epsilon_2 \rangle$ spectra in Fig. 2). These are known Wannier-Mott-like excitons that have been studied in detail before.¹⁰ Outside the visible spectral range there are a few more spectral features of the optical response that appear in the energy range from 8 eV to 18 eV as reported from a synchrotron-radiation-based variable angle ellipsometry measurement.

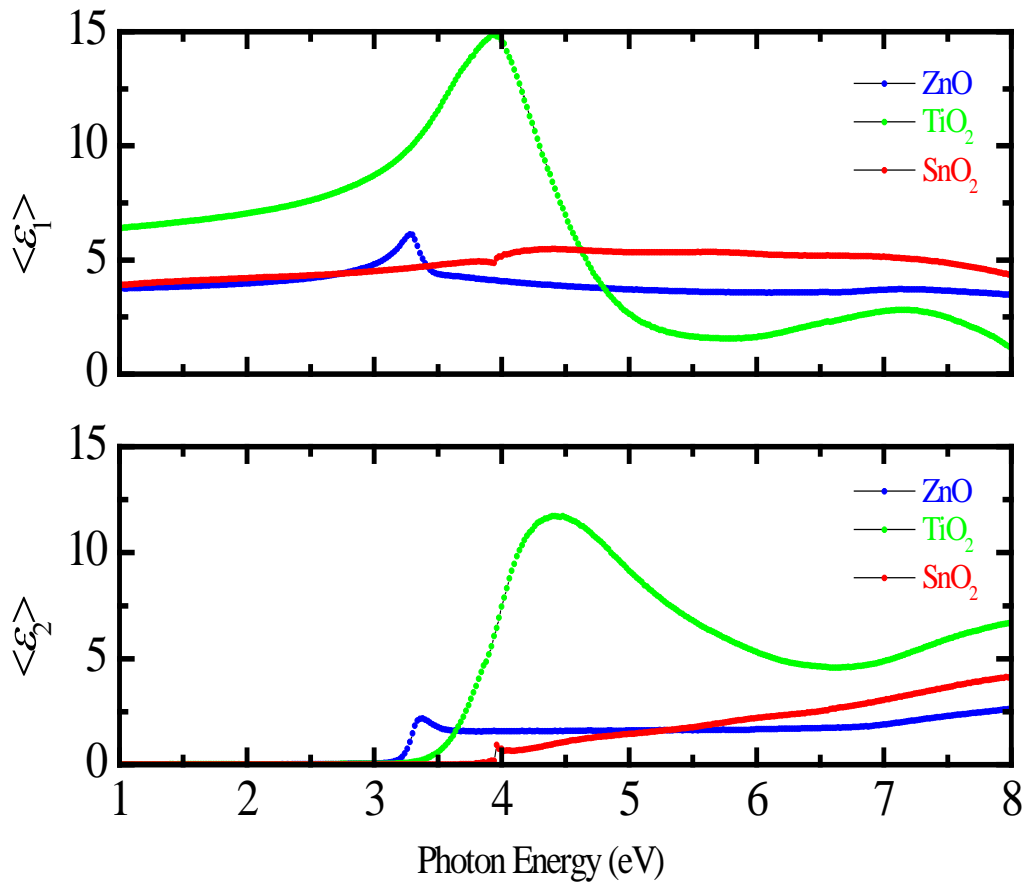


Fig. 2: Real $\langle \epsilon_1 \rangle$ and imaginary $\langle \epsilon_2 \rangle$ parts of the pseudo-dielectric function of ZnO, TiO₂, and SnO₂ determined by VUV spectroscopic ellipsometry.

The optical absorption, $\alpha = 4\pi k/\lambda$, was calculated as a function of photon wavelength λ . From linear fitting to α near the absorption edge,⁴ we obtained the optical bandgaps E_g of ZnO, TiO₂, and SnO₂ to be 3.13 ± 0.05 eV, 3.30 ± 0.05 eV, and 3.95 ± 0.05 eV, respectively, as shown in Fig. 3. The optical band gap of ZnO films has been reported to vary from ~ 3.0 eV to ~ 3.3 eV depending on preparation methods and film morphology.¹¹ In our PLD films growth, the optical band gap is found at 3.13 eV with the appearance of a relatively sharp absorption edge indicating that our PLD ZnO film has a high crystalline quality and is a direct bandgap type. For comparison, in an earlier study,¹² three different values of ~ 3.1 eV, 3.2 eV, and 3.3 eV have been reported for the optical band gap of zinc oxide single crystals at room temperature. Bulk TiO₂ with the principal polymorphs have band gaps in the range of 3.05 - 3.18 eV. Our PLD TiO₂ epitaxial film that might contain different crystal phases (anatase, brookite and rutile) of bulk TiO₂ has a slightly larger bandgap of 3.3 eV and a long band-edge tail that suggests an indirect gap. The assignment of whether TiO₂ is a direct or indirect gap appears to depend on crystal structures and the theoretical predictions seem to divert with different conclusions. Reported experimental and theoretical studies show the feature found at 3.14 eV corresponds with an indirect transition most probably associated with a crystal field or spin-orbit structure of the valence band.¹³ It is worth to point out that the absorption band edge of TiO₂ nanostructures has been found at 3.34 eV and shown to blue-shift from the bulk band edge of 3.19 eV,¹⁴ and the presence of point defects or the simultaneous absorption of a photon and scattering with a phonon can significantly affect the optical properties of TiO₂.¹⁵ In rutile, detailed investigations of the optical absorption edge reveal an indirect transition induced by phonon–exciton interactions.¹⁶ In another theoretical consideration, it showed that rutile TiO₂ form has an indirect band gap of 3.23 eV with the valence band maximum (VBM) at Γ point and the conduction band minimum (CBM) at R point in momentum space. However, in a different study that applies GW approximation, TiO₂ was reported to have an indirect band gap at 3.34 eV and a direct band gap at 3.38 eV.¹⁷ It is worth making a notice that the broad peak at about 5 eV in the TiO₂ absorption (Fig. 2) has been observed in bulk anatase but not in rutile.¹⁸ For SnO₂, the film is highly transparent in the visible spectral range. First principles calculations reveal that the bottom most conduction bands are highly dispersive for SnO₂ polymorphs, which explains their small effective electron masses and the weak optical absorption near the band gap as seen in our PLD SnO₂ absorption (Fig. 3).¹⁹ Our SnO₂ epitaxial film band gap value of 3.95 eV appears to be an average of varied band gaps of single crystal SnO₂ optical anisotropy if we take into account of the direct transitions in undoped or lowly doped SnO₂ crystals which have a band gap of 3.57 eV (3.7 eV) and 3.93 eV (4.1 eV) for light polarized perpendicular (parallel) to the *c*-axis due to optical uniaxial nature of the crystal.²⁰

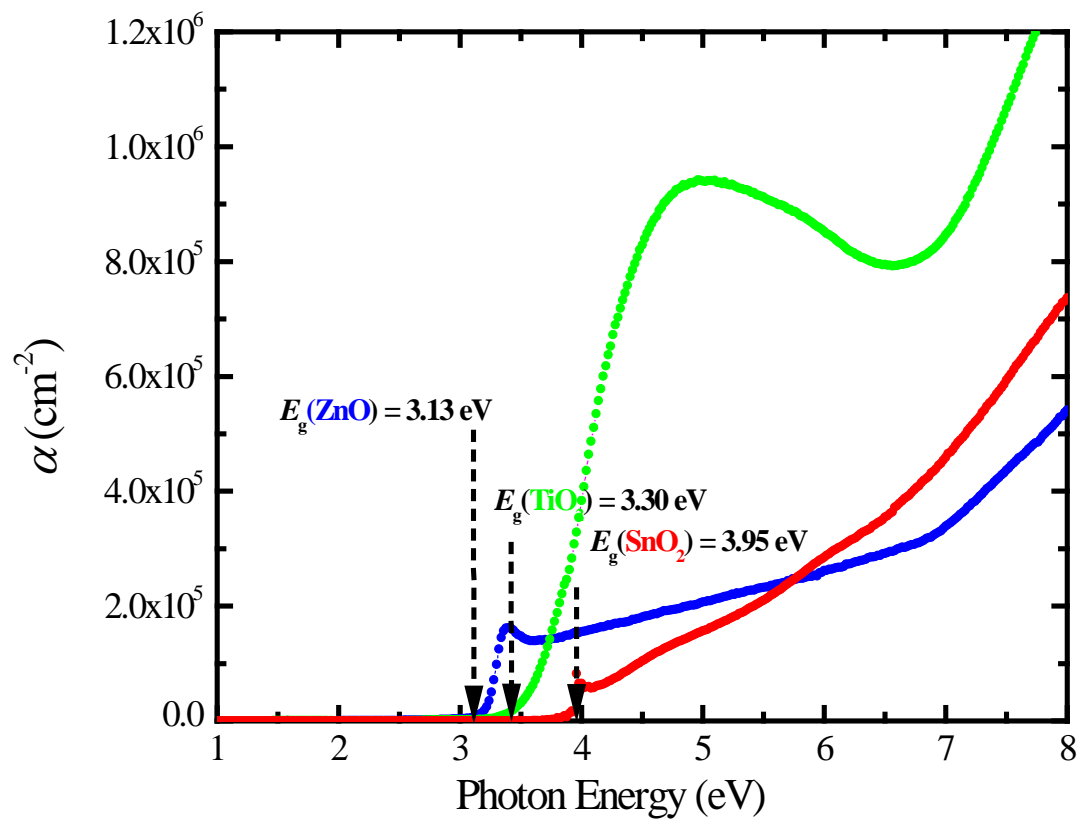


Fig. 3. Absorption calculated from the dielectric functions (Fig. 2) measured by spectroscopic ellipsometry

Within 1.0 eV of the threshold, in general, IPE yield can be approximately expressed in the form of $Y = A (hv - \Phi_F)^\beta$, where hv and Φ_F are the photon energy and the barrier height, respectively, and A is a constant. The exponent β is a phenomenological parameter with a value depending on the density of states at the interface. β was found to commonly equal to $1/2$ for photo-injection from a metal and $1/3$ from a semiconductor.⁸ In the analysis of IPE data for electron photoemitted from the metal oxide layer, we have considered two scenarios of whether to assign the photoelectron transition from the valence band maximum (VBM) or the unintentionally-n doped Fermi level (E_F) of the metal oxide to the conduction band minimum (CBM) of Al_2O_3 . As it turned out, the analysis using VBM of the metal oxides to CBM of Al_2O_3 results in the work function of the metal oxides in the range of 2.0 – 3.0 eV which is unreasonable and much lower than the known values between 5-7 eV. Therefore, the band offsets between our metal oxide films and Al_2O_3 were determined based on the assumption that the electron photoemission injected from the Fermi level inside the naturally doped metal oxide conduction band to the conduction band minimum of Al_2O_3 . Fig. 4 displays the square root of the IPE yield, $Y^{1/2}$, as a function of photon energy, measured at different negative bias, V_g , applied to the back side (RuO_2) of sample ZnO. The photoemission barrier heights, $\Phi_{F [ZnO/Al_2O_3]}$, were determined by linear fitting of $Y^{1/2}$ to photon energy (hv) near the photoemission threshold. The determined Φ_F at different biases (V_g) or internal electric field (F), are seen to have a small difference thus suggesting there is a small field dependence. Similar spectra were obtained for sample SnO_2 and TiO_2 (not shown). The zero-field barrier heights, Φ_0 , or barrier heights at zero-field were deduced from the Schottky plots by linear fitting the barrier heights to the square root of internal electric field. As a result, Fig. 5 shows $\Phi_{0 [SnO_2/Al_2O_3]} = 4.31$ eV, $\Phi_{0 [ZnO/Al_2O_3]} = 4.57$ eV, and $\Phi_{0 [TiO_2/Al_2O_3]} = 4.61$ eV being zero-field barrier heights, Φ_0 , of SnO_2 , ZnO, and TiO_2 , respectively. Only by doping, either by intrinsic defects or by adding dopants, these oxides become conductive. The natural n -type conductivity in ZnO thin films mainly controlled by electrons generated by oxygen vacancies and charge donation gives rise to the Fermi level in the conduction band. In SnO_2 , the conductivity is attributed to oxygen vacancies acting as doubly ionized donors or tin interstitials. Similarly, the formations of intrinsic n -type defects, that is, oxygen vacancies and titanium interstitials, are found in TiO_2 .²¹ Therefore, we assume that our naturally doped PLD films are n -type and doped by the defect formed by oxygen and metal element vacancies. As a result, the electron concentration at the Fermi levels in their conduction bands is responsible for the photoemission. With respect to Al_2O_3 electron affinity of ~ 1.8 eV, the work functions of these PLD metal oxides were estimated to be ~ 6.1 eV, 6.4 eV, and 6.4 eV for SnO_2 , ZnO, and TiO_2 , respectively (see the band diagram in Fig. 5). These estimates appear to be feasible when considering there is broad inconsistency in the work function values reported for many transition metal oxides. The large variation is mainly due to the many different sample

preparation methods.²² For the electron photoemission from Al top contact, the field (F)- dependent barrier heights, $\Phi_{F\text{ [Al/Al}_2\text{O}_3\text{]}}$, from the Fermi level of Al to the bottom of Al₂O₃ conduction band at the interface of Al/Al₂O₃ in three samples were obtained from linear fitting of $Y^{1/2}$ to photon energy (eV) for each spectrum taken at each different bias (V_g) or internal field (F). $\Phi_{0\text{ [Al/Al}_2\text{O}_3\text{]}}$, the *zero*-field barrier height, is extracted by linear fitting of the field-dependent barrier heights $\Phi_{F\text{ [Al/Al}_2\text{O}_3\text{]}}$ to the internal electrical field (F) using Schottky plots in Fig. 5 for all three samples. As a result, $\Phi_{0\text{ [Al/Al}_2\text{O}_3\text{]}}$ was found to be 3.07 eV, 3.05 eV, and 2.95 eV for the case of ZnO, TiO₂, and SnO₂, each underneath Al₂O₃ layer, respectively, and averaged to 3.02 eV which is in a good agreement with the published values.^{9,23}

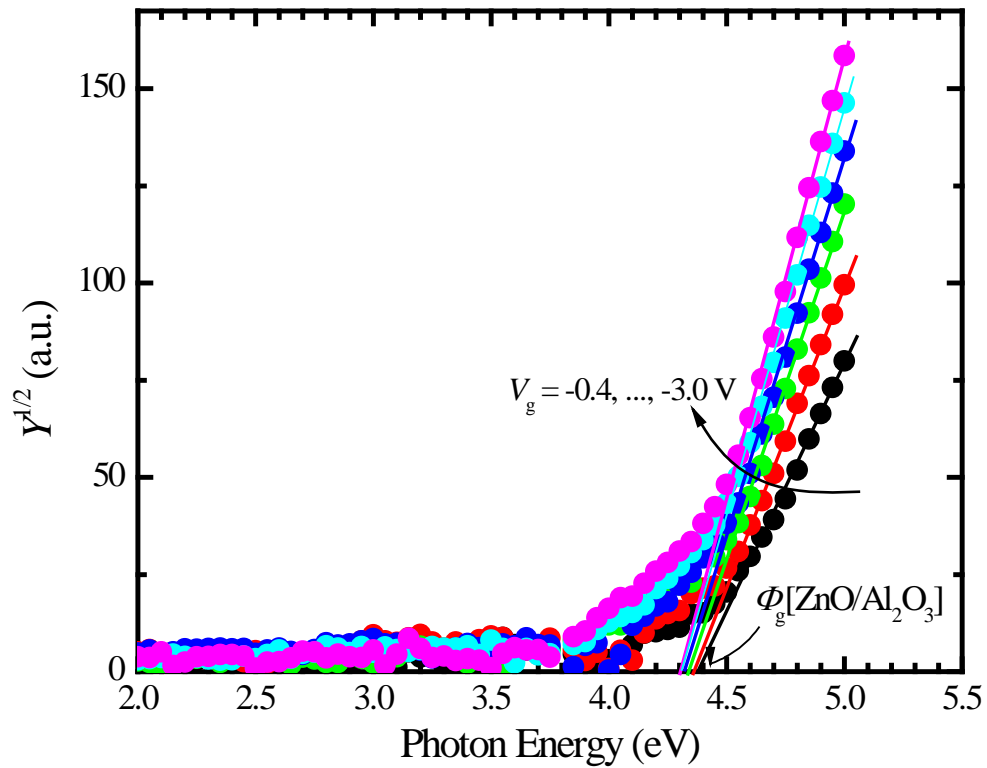


Fig. 4. Square root of yield Y at various negative biases V_g applied between the top contact Al and the back contact RuO_2 . Linear fits to $Y^{1/2}$ near the spectral thresholds determine the barrier heights at the metal oxide / Al_2O_3 interface, shown here for ZnO.

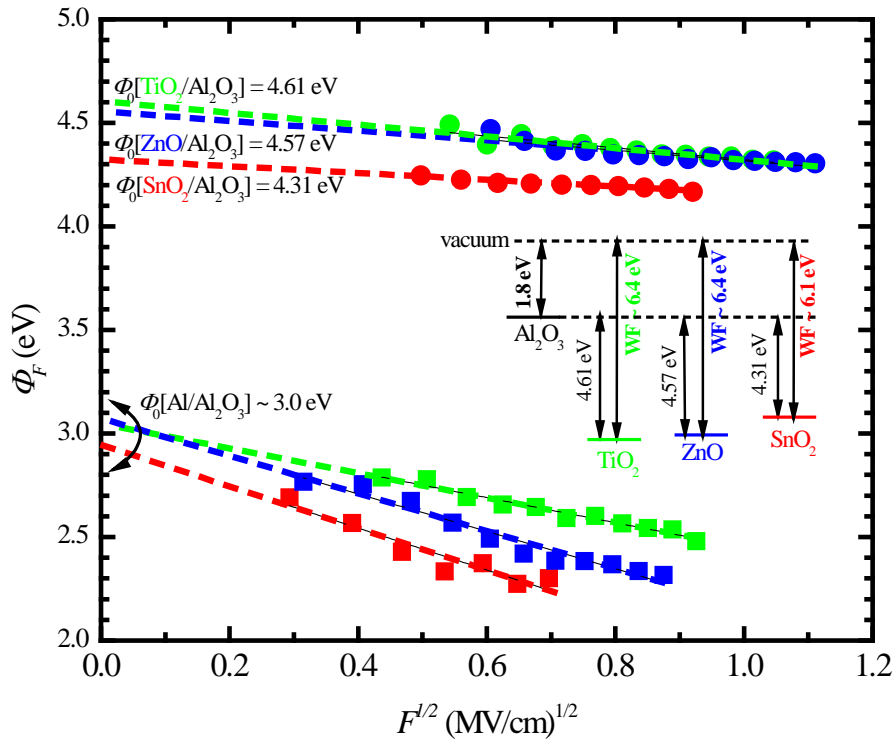


Figure 5. Schottky plots used to determine the barrier height at the zero-field (Φ_0) or the flat band condition. Inset is the band diagram (not to scale) showing the work functions (WF's) which are the sum of electron affinity (1.8 eV) of Al₂O₃ and the zero-field barrier heights of the metal oxides determined by internal photoemission (see text).

In summary, using vacuum ultra-violet spectroscopic ellipsometry we investigated the optical properties of TiO₂, ZnO, and SnO₂, deposited by pulse laser deposition and determined the optical band gaps to be 3.30 ± 0.05 eV, 3.13 ± 0.05 eV, and 3.95 ± 0.05 eV, respectively. SnO₂ and ZnO spectral optical responses near the band gap reveal that they are a direct optical band gap, and on the other hand, TiO₂ appears to be indirect. For the interfacial electronic characteristics, internal photoemission measurements show that, at the interface of naturally doped (unintentionally doped) metal oxide and Al₂O₃, the electron photoemission originates from the Fermi level in the conduction band of the metal oxide to the conduction band of Al₂O₃. From the measured energy barrier heights, the work functions of these metal oxides were estimated and found to be consistent with reported values. Furthermore, this study demonstrates that internal photoemission spectroscopy can be extended to characterize electronic interfacial properties of other transparent conducting oxide materials.

References

- ¹ D. S. Ginley, H. Hosono and D. C. Paine, *Handbook of Transparent Conductors* (Springer, 2010).
- ² P. P. Edwards, A. Porch, M. O. Jones, D. V. Morgan, and R. M. Perks, *Dalton Trans.* **19**, 2995 (2004).
- ³ J. E. Medvedeva and A. J. Freeman, *Europhys. Lett.* **69**, 583 (2005).
- ⁴ Klaus Ellmer, Rainald Mientus, and Stefan Seeger, *Transparent Conductive Materials: Materials, Synthesis, Characterization, Applications*, 1st Ed, Edited by David Levy and Erick Castellón, Chapter 2, 33 (Wiley-VCH Verlag GmbH & Co. KGaA., 2018).
- ⁵ Chrisey B. Douglas and Hubler K. Graham, *Pulsed Laser Deposition of Thin Film* (John Wiley & Sons, 1994).
- ⁶ Yong Jai Cho, N. V. Nguyen, C. A. Richter, J. R. Ehrstein, Byoung Hun Lee, and Jack C. Lee, *Appl. Phys. Lett.* **80**, 1249 (2002).
- ⁷ S. C. Dixon, D. O. Scanlon, C. J. Carmalt, and I. P. Parkin, *J. Mater. Chem. C* **4**, 6946 (2016); D.O. Scanlon and G. W. Watson, *J. Mater. Chem.* **22**, 25236 (2012).
- ⁸ V. V. Afanas'ev, *Internal Photoemission Spectroscopy: Principles and Applications* (Elsevier, Amsterdam, 2008).
- ⁹ K. Xu, H. Sio, O. A. Kirillov, L. Dong, M. Xu, P. D. Ye, D. Gundlach, and N. V. Nguyen¹, *J. App. Phys.* **113**, 024504 (2013).
- ¹⁰ R. Laskowski and N. E. Christensen, *Phys. Rev. B* **73**, 045201 (2006); A. Schleife, C. Rödl, F. Fuchs, J. Furthmüller, and F. Bechstedt, *Appl. Phys. Lett.* **91**, 241915 (2007).
- ¹¹ Mursal, Irhamni, Bukhari, and Zulkarnain Jalil, *J. of Phys.: Conf. Series* **1116**, 032020 (2018).
- ¹² V. Srikant and D. R. Clarke, *J. of Appl. Phys.* **83**, 5447 (1998).
- ¹³ J. Pascual, J. Camassel, and H. Mathieu, *Phys. Rev. B* **18**, 5606 (1978)
- ¹⁴ Nosipho Moloto, Siyasanga Mpelane, Lucky M Sikhwivhilu, Suprakas Sinha Ray, *Int. J. Photoenergy* **2012**, 1 (2012).
- ¹⁵ T. Sekiya, S. Ohta, S. Kamei, M. Hanakawa, S. Kurita, *J. Phys. Chem. Solids* **62**, 717 (2001).
- ¹⁶ A. E. Goresy, M. Chen, P. Gillet, L. Dubrovinsky, G. Graup, *Earth Planet. Sci. Lett.* **192**, 485 (2001).
- ¹⁷ W. Kang and M. S. Hybertsen, *Phys. Rev. B* **82**, 085203 (2010).
- ¹⁸ T. E. Tiwald, M. Schubert, *Proc. SPIE* **4103**, 19 (2000); N. Hosaka, T. Sekiya, C. Satoko, S. Kurita, *J. Phys. Soc. Jpn.* **66**, 877 (1997).
- ¹⁹ M. Douand and C. Persson, *J. Appl. Phys.* **113**, 083703(2013).
- ²⁰ A. Schleife, J. B. Varley, F. Fuchs, C. Rodl, F. Bechstedt, P. Rinke, A. Janotti, and C. G. Van De Walle, *Phys. Rev. B - Condens. Matter* **83**, 35116 (2011).

-
- ²¹ Benjamin J. Morgan and Graeme W. Watson, *J. Phys. Chem. C* **114**, 2321 (2010).
- ²² Mark T. Greiner, Lily Chai, Michael G. Helander , Wing-Man Tang , and Zheng-Hong Lu. *Adv. Funct. Mater.* **22**, 4557 (2012).
- ²³ V. V. Afanas'ev, M. Houssa, and A. Stesmans, *J. Appl. Phys.* **91**, 3079 (2002).